

1 **Title**

2 **Functional characterization of ovine dorsal root ganglion neurons reveals peripheral**
3 **sensitization after osteochondral defect.**

4

5 **Authors**

6 Sampurna Chakrabarti^{1,2,4}, Minji Ai^{3,4}, Wai Ying Katherine Wong², Karin Newell³, Frances
7 M.D. Henson^{*3}, Ewan St. John Smith^{2*}.

8 **Email addresses:**

9 Sampurna.chakrabarti@mdc-berlin.de, ma839@cam.ac.uk, wykw2@cam.ac.uk,
10 kjr20@cam.ac.uk, fmdh1@cam.ac.uk, es336@cam.ac.uk.

11 **Affiliations**

12 ¹ Department of Neuroscience, Max-Delbrück-Centrum für Molekulare Medizin (MDC).
13 Berlin, Germany.

14 ² Department of Pharmacology, University of Cambridge, UK.

15 ³ Department of Veterinary Medicine, University of Cambridge, UK.

16 ⁴ These authors contributed equally

17 *Corresponding authors: Ewan St. John Smith, Department of Pharmacology, University of
18 Cambridge, Tennis Court Road, Cambridge CB2 1PD, United Kingdom, Email:
19 es336@cam.ac.uk.

20 Frances M.D. Henson, Division of Trauma and Orthopaedic Surgery, Department of Surgery,
21 University of Cambridge, Box 202, Addenbrooke's Hospital, Hill's Rd, Cambridge CB2 0QQ,
22 UK. Email: fmdh1@cam.ac.uk

23 **Abstract (limit: 250 words)**

24 Objective: Knee joint trauma can cause an osteochondral defect (OD), a risk factor for
25 osteoarthritis and cause of debilitating pain in patients. Modelling OD in rodents is difficult
26 due to their smaller joint size. This study proposes sheep as a translationally relevant model to
27 understand the neuronal basis of OD pain.

28 Methods: Unilateral 6 mm deep OD was induced in adult sheep, 2-6 weeks after which dorsal
29 root ganglion neurons (DRG neurons) were cultured from the control and OD side. Functional
30 assessment of neuronal excitability and activity of the pain-related ion channels, TRPV1 and
31 P2X3, was carried out using electrophysiology and Ca²⁺-imaging. Immunohistochemistry was
32 utilized to verify expression of pain-related proteins.

33 Results: An increased proportion of OD DRG neurons (sheep, n = 3, Ctrl neurons, n =15, OD
34 neurons, n = 16) showed spontaneous electrical excitability (p = 0.009, unpaired t-test) and
35 hyperexcitability upon TRPV1 agonist (capsaicin) application (p = 0.04, chi-sq test). Capsaicin
36 also produced Ca²⁺ influx in an increased proportion of OD DRG neurons isolated (p = 0.001,
37 chi-sq test). By contrast, neither protein expression, nor functionality of the P2X3 ion channel
38 were altered in OD neurons.

39 Conclusions: We provide evidence of increased excitability of DRG neurons (which is an
40 important neural correlate of pain) and TRPV1 function in an OD sheep model. Our data show
41 that functional assessment of sheep DRG neurons can provide important insights into the neural
42 basis of OD pain and thus potentially prevent its progression into arthritic pain.

43 **Keywords: Pain, sheep model, osteochondral defect, neuron, knee**

44 **Introduction**

45 Osteochondral lesions are detected in ~60% of patients who undergo knee arthroscopies¹.
46 Clinically, osteochondral defects (OD) constitute damage to bones (osteo) and cartilage
47 (chondral) and commonly present as pain and swelling of joints after an acute injury, initial
48 radiographs often being negative for lesions². OD is diagnosed only if pain on weight bearing
49 persists for more than 4-6 weeks post-injury and can also reduce the quality of life of patients
50 to a similar extent to individuals with late stage osteoarthritis (OA)^{1,2}. Indeed, OD in adults is
51 a risk factor for progression to OA, highlighting the importance of OD research as prevention
52 for OA progression³. In OD, pain is suspected to arise from hyperexcitability of sensory nerves
53 innervating the subchondral bone which is further amplified by secretion of inflammatory
54 mediators from the aneural articular cartilage and synovial membrane³. However, direct
55 evidence of sensory nerve hyperexcitability in OD and the mechanisms involved in such
56 peripheral sensitization is lacking.

57 Peripheral sensitization is commonly studied by electrophysiological recordings of isolated
58 dorsal root ganglion neurons (DRG, location of the cell bodies of sensory nerves innervating
59 the body, but not the head) harvested from rodents. However, rodent models of OD are difficult
60 to create and less translatable because of their smaller cartilage volume (rats: 2.17 mm³)
61 compared to humans (552 mm³)⁴. The thinner cartilage in rodents restricts the amount of
62 damage that can be induced, and therefore is less translatable to the human disease. In contrast,
63 large animals, such as sheep, have a similar cartilage volume (359 mm³) to humans and OD
64 can successfully be induced in their joints as evidenced by histological scoring and reduced
65 activity^{4,5}. Consequently, the majority of OD research is focused on developing strategies for
66 bone and cartilage regeneration, such as implantation of biomaterials in large animal models⁴.
67 Whether such regeneration strategies also decrease any neuronal sensitization that occurs in

68 OD, and hence pain, is largely unknown due to the lack of expertise in isolation and recording
69 of DRG neurons from large animals.

70 In this study, we provide the first evidence of peripheral sensitization in an OD model of the
71 sheep stifle joint by electrophysiological recording and Ca²⁺ imaging of isolated DRG neurons.
72 Such an in vitro experimental paradigm could be utilized to identify translatable pain targets
73 for OD and OA and as an outcome measure of future pain therapeutics and cartilage
74 regeneration technologies.

75 **Material and methods**

76 This study was approved by the University of Cambridge Animal Welfare and Ethical Review
77 Body and the UK Home Office (Project License 70/8165). See supplementary file for detailed
78 methodology.

79

80 *Animals*

81 Six skeletally mature female Welsh Mountain sheep (3.2 ± 0.8 years, 40-44kg) housed in
82 flocks under natural conditions with the same feed, husbandry and location were included in
83 the study. A 6-mm deep, 8-mm wide OD was created using a hand drill on the left stifle joint
84 of these sheep under anesthesia (thiopentone, 3 mg/kg intravenous, followed by isoflurane),
85 accompanied by analgesia (carprofen, 4 mg/kg, intramuscular) and prophylactic antibiotic
86 administration (procain penicillin). Animals were sacrificed by injection of 40 ml 20% (w/v,
87 intravenous.) pentobarbitone sodium at 2, 4, and 6 weeks post-surgery. A semiquantitative
88 histological analysis using International Cartilage Repair Society macroscopic score was
89 carried out blindly as previously established⁵.

90

91 *DRG neuron isolation and culture*

92 L3 – L4 DRG from control and OD sides of sheep were collected after transection of vertebral
93 bodies from the lumbar region in ice cold dissociation media as described before^{6,7}. The
94 collected DRG were cut into ~ 3 mm³ pieces before enzymatic digestion with collagenase
95 followed by trypsin (1mg/ml each). The DRG were then kept in trypsin and collagenase
96 digestion solutions for ~ 30 min each, including a 5-10 min shaking step at the beginning of
97 incubation; before mechanical trituration and plating on Poly-D-lysine and laminin coated

98 glass bottomed dishes (MatTek, P35GC-1.5-14-C). Plated neurons were incubated at 37 °C,
99 5% CO₂.

100

101

102 *Whole-cell patch clamp electrophysiology*

103 DRG neuron recordings were made following overnight incubation. Tested neurons were
104 bathed in extracellular solution (ECS) and recorded from using an EPC-10 amplifier (HEKA)
105 and Patchmaster© software (HEKA). Glass pipettes with a resistance of 3–6 MΩ loaded with
106 intracellular solution (ICS) were used for whole-cell patch clamp. Action potentials (AP) were
107 recorded under current-clamp mode either without current injection (to record spontaneous
108 firing) or following stepwise current injection (to evoke firing). Transient receptor potential
109 vanilloid receptor 1 (TRPV1) and purinergic (P2X3) ion channel agonists (capsaicin (1 μM)
110 and α,β, mATP (30 μM), Sigma) were applied to DRG neurons for 10s to determine their ability
111 to evoke APs under current clamp mode. Current-voltage relationships were obtained using a
112 standard voltage-step protocol under voltage-clamp mode (Figure 1G).

113

114

115 *Ca²⁺ imaging*

116 DRG neurons were incubated in 10 μM of the Ca²⁺ indicator Fluo-4 AM (Invitrogen, UK) for
117 30 min at room temperature (21°C). Neurons were then washed with ECS and placed under a
118 microscope (Nikon Eclipse Tie-S, Nikon) for imaging. Fluro-4 fluorescence was excited by a
119 470 nm LED (Cairn Research) and images were captured by a digital camera (Zyla cSMOS,
120 Andor) at 1 Hz with 50 ms exposure time using Micro-Manager software (v1.4; NIH). 50 mM

121 KCl was used as positive control. Data analysis was conducted using a custom made R toolbox
122 (<https://github.com/amaprums/Calcium-Imaging-Analysis-with-R>).

123

124 *Immunohistochemistry*

125 L3 – L4 DRG from OD and control sides of sheep were collected in Zamboni’s fixative,
126 embedded in Shandon M-1 embedding matrix (Thermo Fisher Scientific, UK), snap frozen and
127 stored at -80°C as described before. One to three 12 µm sections were chosen randomly from
128 both sides for staining as previously established⁶ using an anti-CGRP antibody (1:5000, Sigma
129 C8189, anti-rabbit polyclonal), an anti-P2X3 antibody (1:1000, Alomone APR016, anti-rabbit
130 polyclonal) and an Alexa-488 conjugated secondary antibody (1:1000, Invitrogen A21206).
131 The mean gray value of each DRG neuron was measured in ImageJ and a custom-made R
132 toolkit (https://github.com/amaprums/Immunohistochemistry_Analysis) was used to identify
133 positive neurons with manual validation as previously described⁶.

134

135 *Statistics*

136 Data are shown as mean ± Standard Errors of Mean (SEM). Two group comparisons were
137 made with Student’s unpaired t-test, and percentage comparison was done using a chi-square
138 test. One-way ANOVA (Analysis of Variance) with Tukey’s post-hoc test was used to compare
139 the significance among three groups.

140

141

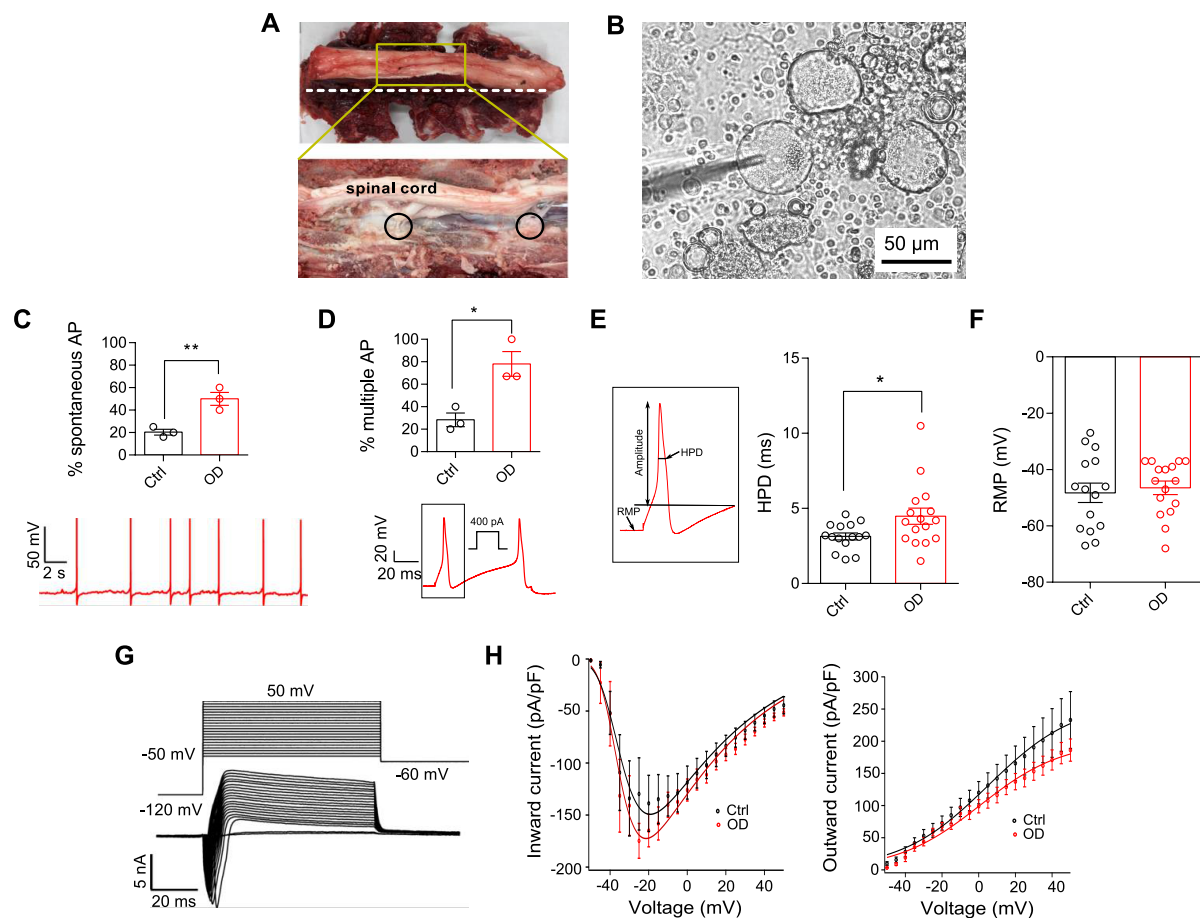
142

143 **Results**

144 **OD induces hyperexcitability in sheep DRG neurons**

145 A 6 mm OD was created unilaterally on the femoral condyle of sheep (n=3) stifle joint which
146 resulted in cartilage damage (assessed macroscopically, Supplementary Table 1). Pain is the
147 major symptom of OD in humans and we have previously reported that synovial fluid from
148 patients with painful OA can increase the excitability of mouse DRG neurons⁸. Consequently,
149 we hypothesized that the isolated DRG neurons from the OD side of sheep would show
150 hyperexcitability. To test this hypothesis, we harvested, cultured and performed patch-clamp
151 recording on the DRG neurons isolated from the ctrl (n = 15) and OD (n = 16) sides of the
152 sheep (Figure 1A). We recorded from small-medium sized putative nociceptors (<1000 μm^2 in
153 area; Figure 1B and Supplementary figure 1) and showed that neurons from the OD side have
154 enhanced spontaneous AP firing in the absence of current injection (p = 0.009, unpaired t-test,
155 Figure 1C) and multiple AP firing (p = 0.01, unpaired t-test, Figure 1D) after current injection.
156 These results suggest that OD enhances excitability of nociceptors. Notably, the AP threshold
157 in both ctrl and OD neurons were ~ 100 pA (Supplementary Table 2), which is lower than that
158 reported for murine neurons⁶. Additionally, AP half-peak duration (HPD) was increased in
159 neurons isolated from the OD side (p = 0.03, unpaired t-test, Figure 1E) although no change in
160 resting membrane potential (RMP) or other AP properties was observed (Figure 1F,
161 Supplementary Table 2). Increased HPD is suggestive of increased voltage-gated Ca^{2+} (Ca_v)
162 and $\text{Na}_v1.8$ channel function⁹, but no difference in inward (mediated by Na_v and Ca_v) or
163 outward (mediated by K_v) current-voltage relationship was found between ctrl and OD
164 conditions (Figure 1G,H), although recordings of isolated Na_v , Ca_v and K_v currents were not
165 conducted. Taken together, our data suggest that 2-6 weeks after OD, sheep DRG neurons show
166 increased excitability, which is a correlate of pain, and this increase in excitability is not due
167 to significant changes in the activity of voltage-gated ion channels.

168



169

170 Figure 1: A) Photo showing intact (top) lumbar region of a sheep spine and after transverse
 171 section (white dotted dissection line, bottom) to expose DRG (black circles). B) Acutely
 172 dissociated sheep DRG neurons in culture. C) Percentage of neurons showing
 173 spontaneous activity in ctrl and OD condition (top) and a representative OD neuron with
 174 spontaneous activity (bottom). D) Percentage of neurons firing multiple action potentials
 175 (AP) upon current injection (top) and a representative trace of multiple firing in response
 176 to 400 pA injected current (bottom). E) Schematic representation of AP properties (left)
 177 and distribution of half peak duration (HPD) (right) and (F) resting membrane potential
 178 (RMP) in ctrl and defect conditions. G) Representative traces of currents evoked from a
 179 neuron at different voltages and (H) plots of the inward and outwards currents in ctrl
 180 (black) and OD (red) neurons. *: $p < 0.05$, **: $p < 0.01$, unpaired t-test.

181

182

183

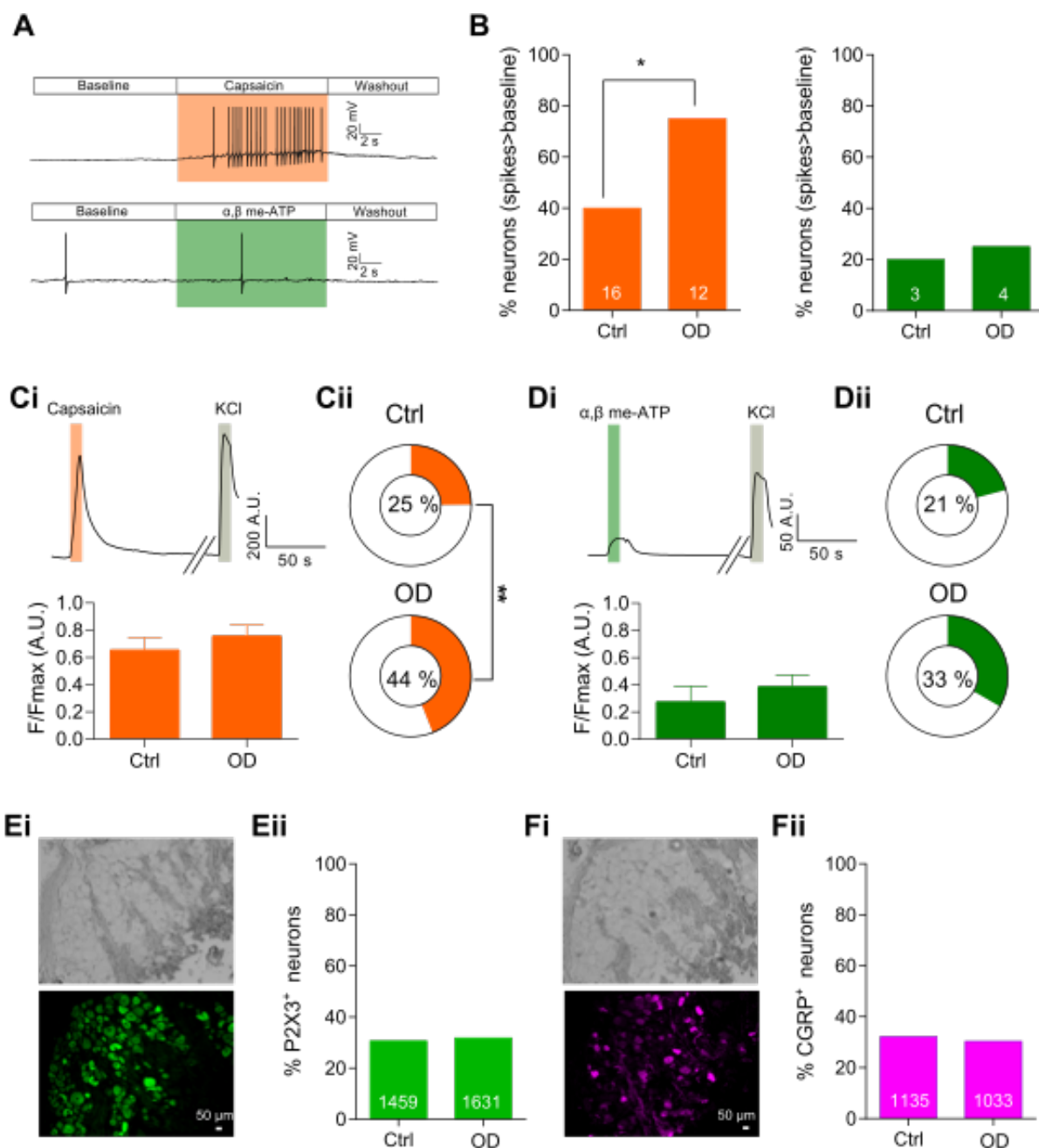
184 **Sheep DRG neurons show increased TRPV1 function after OD**

185 In addition to voltage-gated ion channels, increased functionality of algogen-sensing ion
186 channels can cause nociceptor hyperexcitability¹⁰. We tested agonists of TRPV1 and P2X3 ion
187 channels (capsaicin and α,β me-ATP respectively) and observed that sheep DRG neurons
188 respond to these known algogens by firing AP (Figure 2A) similar to neurons isolated from
189 mouse and human DRG¹⁰. Additionally, we observed that the proportion of OD neurons firing
190 above baseline upon application of capsaicin was significantly higher than the ctrl neurons,
191 implicating an increase in TRPV1 function ($p = 0.04$, chi-sq test, Figure 2B). However, α,β
192 me-ATP produced above baseline firing in a similar proportion of neurons isolated from both
193 control and OD sides, thus arguing against a significant role for P2X3 channel in OD pain
194 (Figure 2B). Next we performed Ca^{2+} -imaging on these neurons to reveal that after OD, an
195 increased proportion of neurons respond to capsaicin (ctrl, 35/141, OD, 48/109, $p = 0.001$, chi-
196 sq test, Figure 2Ci,ii), while the number of neurons responding to α,β me-ATP was not
197 significantly different between ctrl and OD groups (ctrl, 24/115, OD, 23/69, Figure 2Di,ii).
198 Congruently, we showed using IHC on sections of whole DRG that the proportion of P2X3+
199 neurons was similar (~30 %) in ctrl and OD conditions (Figure 2Ei,ii), however, protein level
200 expression of TRPV1 could not be validated due to the unavailability of a specific antibody for
201 sheep TRPV1 (tested antibodies listed in Supplementary Table 3). Finally, we probed the
202 expression of the pro-nociceptive neuropeptide, CGRP, in DRG sections because an increase
203 in TRPV1 expression can in turn induce production of CGRP¹¹. However, the CGRP+ neurons
204 were ~30% in both OD and ctrl conditions (as observed before⁷) suggesting that the proportion
205 of peptidergic CGRP neurons is unchanged in OD pain (Figure 2Fi,ii).

206 Taken together our data provide support that OD causes hyperexcitability of sheep DRG
207 neurons and that increased function of TRPV1 is part of the sensitization process. Since TRPV1

208 is also an important pain target in OA, TRPV1 antagonists utilized for pain-control in OD
 209 might also help prevent pain in cases of OD that develop into OA.

210



211

212 Figure 2: A) Patch-clamp traces showing a representative DRG neuron from the ctrl side firing
 213 AP spikes above baseline and same as baseline in response to capsaicin and α, β me-
 214 ATP respectively. B) Bar graph showing percentage of neurons with above baseline
 215 firing activity in response to capsaicin (left, orange) and α, β me-ATP (right, green).

216 Numbers on the bars represent number of neurons in each condition firing above
217 baseline. Ci) (top) Representative Ca^{2+} trace from a neuron responding to capsaicin and
218 KCl (positive control). (bottom) Magnitude of Ca^{2+} influx in response to capsaicin (ctrl,
219 $n = 35$, defect, $n = 48$). Cii) Percentage of neurons responding to capsaicin in each
220 condition. Di) (top) Representative Ca^{2+} trace from a neuron responding to α,β me-ATP
221 and KCl (positive control), (bottom) magnitude of Ca^{2+} influx in response to α,β me-
222 ATP (ctrl, $n = 24$, defect, $n = 23$). Dii) Percentage of neurons responding to α,β me-
223 ATP in each condition. Ei) Representative brightfield (top) and anti-P2X3-antibody
224 stained (bottom) image of a whole sheep DRG in cross-section along with the percentage
225 of neurons positive for P2X3 (Eii). Fi) Representative brightfield (top) and anti-CGRP-
226 antibody stained (bottom) image of a whole sheep DRG in cross-section along with the
227 percentage of neurons positive for CGRP (Fii). Numbers on the bars represent neurons
228 positive for the respective antibody staining. *: $p < 0.05$, **: $p < 0.01$, chi-sq test.

229

230 **Discussion**

231 We have previously proposed that large animals, such as sheep, can be leveraged as
232 translational models to investigate mechanisms of joint pain in vitro due to their larger joint
233 anatomy and DRG neuron diameter compared to rodents¹². In this study we provide proof using
234 the ovine OD model (which is difficult to induce in rodents) that it is possible to study neuronal
235 constructs of peripheral sensitization in large animals using tools developed for rodent DRG
236 neurons. For example, we show using whole-cell patch clamp electrophysiology and Ca^{2+} -
237 imaging that sheep DRG neurons can be activated by agonists of nociceptive ion channels
238 TRPV1 and P2X3, thus indicating their functional presence.

239

240 Importantly, we found using whole-cell patch clamp that an increased proportion of OD
241 neurons fired spontaneous AP, as well as multiple APs within 80 ms in response to injected
242 current. The increase in AP firing was not associated with significant changes in voltage-gated
243 ion channel activity, however, further studies are needed to determine changes in the function

244 of hyperpolarization-activated cyclic nucleotide-gated channels, which have been implicated
245 in sensory nerve firing and pain¹³. We also observed increased AP firing upon administration
246 of the TRPV1 agonist capsaicin in OD neurons, along with an increased proportion of OD
247 neurons responding to capsaicin using Ca²⁺-imaging assay. These data suggest that TRPV1-
248 mediated depolarization can increase AP firing in sensory neurons to a greater extent after OD,
249 which is consistent with mechanistic studies showing a TRPV1-anoctamin 1 interaction that
250 increases prolonged glutamate release to induce pain-related behaviors¹⁴. Furthermore, our data
251 are consistent with peripheral sensitization observed in models of joint pain⁶, implying that
252 similar nociceptive mechanisms are also at play before induction of arthritis. Therefore,
253 TRPV1 antagonists have the potential to ameliorate or perhaps prevent onset of arthritic pain.

254

255 Lastly, we observed that expression of CGRP and P2X3, markers of peptidergic and non-
256 peptidergic sensory neurons respectively, were mostly expressed in small-size DRG neurons
257 (<1000 μm^2 , Supplementary Figure 1) in a similar manner to in rodent and human DRG¹⁵.
258 Additionally, the lack of change in the percentage of neurons expressing P2X3 correlates with
259 our observation that P2X3 function remained unchanged after OD.

260

261 This study highlights that sheep have huge, hitherto untapped, potential in mechanistic joint
262 pain research. However, efforts need to be made to develop tools effective for large animals.
263 For example, due to the unavailability of specific antibodies that work on sheep tissue, we were
264 unable to assess using IHC if enhanced TRPV1 expression occurred in DRG neurons, as well
265 as being unable to investigate if P2X3 and CGRP are coexpressed a subset of DRG neurons as
266 has been observed in human DRG¹⁵. Nevertheless, our study paves the way for future
267 investigation of pain mechanisms in OD which might help prevent progression of joint trauma
268 to arthritis.

269 **Contributions:** S.C. designed and conducted experiments, analyzed data and wrote the
270 manuscript. M.A. conducted experiments, analyzed data and wrote the paper. K.W. conducted
271 experiments and analyzed data. K.N. conducted experiments and analyzed data. F.M.D.H. and
272 E.S.J.S designed experiments and revised the manuscript. All authors approve the final form
273 of the article.

274 **Funding sources:** S.C. was supported by the Gates Cambridge Trust scholarship. This work
275 was supported by funding from Versus Arthritis (RG21973) and BBSRC (BB/R006210/1) to
276 E.St.J.S and Horizon 2020 (RG90905) and Innovate UK (RG87266) to F.M.D.H.

277 **Competing interests:** The authors declare no competing interest.

278 **References**

- 279 1. Katagiri H, Mendes LF, Luyten FP. Definition of a Critical Size Osteochondral Knee
280 Defect and its Negative Effect on the Surrounding Articular Cartilage in the Rat.
281 *Osteoarthritis Cartilage*. 2017;25(9):1531-1540. doi:10.1016/j.joca.2017.05.006
- 282 2. van Dijk CN, Reilingh ML, Zengerink M, van Bergen CJA. Osteochondral defects in
283 the ankle: why painful? *Knee Surg Sports Traumatol Arthrosc*. 2010;18(5):570-580.
284 doi:10.1007/s00167-010-1064-x
- 285 3. Lepage SIM, Robson N, Gilmore H, et al. Beyond Cartilage Repair: The Role of the
286 Osteochondral Unit in Joint Health and Disease. *Tissue Eng Part B Rev*.
287 2019;25(2):114-125. doi:10.1089/ten.TEB.2018.0122
- 288 4. Meng X, Ziadlou R, Grad S, et al. Animal Models of Osteochondral Defect for Testing
289 Biomaterials. *Biochem Res Int*. 2020;2020:9659412-9659412.
290 doi:10.1155/2020/9659412
- 291 5. Newell K, Chitty J, Henson FM. "Patient reported outcomes" following experimental
292 surgery-using telemetry to assess movement in experimental ovine models. *Journal of*
293 *orthopaedic research : official publication of the Orthopaedic Research Society*.
294 2018;36(5):1498-1507. doi:10.1002/jor.23790
- 295 6. Chakrabarti S, Pattison LA, Singhal K, Hockley JRF, Callejo G, Smith ESJ. Acute
296 inflammation sensitizes knee-innervating sensory neurons and decreases mouse digging
297 behavior in a TRPV1-dependent manner. *Neuropharmacology*. 2018;143(June):49-62.
298 doi:10.1016/j.neuropharm.2018.09.014
- 299 7. Russo D, Clavenzani P, Mazzoni M, Chiocchetti R, Di Guardo G, Lalatta-Costerbosa G.
300 Immunohistochemical characterization of TH13-L2 spinal ganglia neurons in sheep
301 (*Ovis aries*). *Microscopy Research and Technique*. 2010;73(2):128-139.
302 doi:10.1002/jemt.20764

- 303 8. Chakrabarti S, Jadon DR, Bulmer DC, Smith EStJ. Human osteoarthritic synovial fluid
304 increases excitability of mouse dorsal root ganglion sensory neurons: an in-vitro
305 translational model to study arthritic pain. *Rheumatology*. 2020;59(3):662-667.
306 doi:10.1093/rheumatology/kez331
- 307 9. Blair NT, Bean BP. Roles of Tetrodotoxin (TTX)-Sensitive Na⁺ Current, TTX-
308 Resistant Na⁺ Current, and Ca²⁺ Current in the Action Potentials of Nociceptive
309 Sensory Neurons. *J Neurosci*. 2002;22(23):10277.
- 310 10. Davidson S, Copits BA, Zhang J, Page G, Ghetti A, Gereau RW. Human sensory
311 neurons: Membrane properties and sensitization by inflammatory mediators. *Pain*.
312 2014;155(9):1861-1870. doi:10.1016/j.pain.2014.06.017
- 313 11. Iyengar S, Ossipov MH, Johnson KW. The role of calcitonin gene-related peptide in
314 peripheral and central pain mechanisms including migraine. *Pain*. Published online
315 2017. doi:10.1097/j.pain.0000000000000831
- 316 12. Chakrabarti S, Ai M, Henson FMD, Smith EStJ. Peripheral mechanisms of arthritic
317 pain: A proposal to leverage large animals for in vitro studies. *Neurobiology of Pain*.
318 2020;8:100051. doi:10.1016/j.ynpai.2020.100051
- 319 13. Tsantoulas C, Láinez S, Wong S, Mehta I, Vilar B, McNaughton PA.
320 Hyperpolarization-activated cyclic nucleotide-gated 2 (HCN2) ion channels drive pain
321 in mouse models of diabetic neuropathy. *Sci Transl Med*. 2017;9(409):eaam6072-
322 eaam6072. doi:10.1126/scitranslmed.aam6072
- 323 14. Takayama Y, Uta D, Furue H, Tominaga M. Pain-enhancing mechanism through
324 interaction between TRPV1 and anoctamin 1 in sensory neurons. *Proc Natl Acad Sci*
325 *USA*. 2015;112(16):5213. doi:10.1073/pnas.1421507112
- 326 15. Ray P, Torck A, Quigley L, et al. Comparative transcriptome profiling of the human and
327 mouse dorsal root ganglia: an RNA-seq-based resource for pain and sensory
328 neuroscience research. *Pain*. 2018;159(7):1325-1345.
329 doi:10.1097/j.pain.0000000000001217

330

331 **Extended Material and methods**

332 This study is approved by the University of Cambridge Animal Welfare and Ethical Review
333 Body (AWERB) and the UK Home Office (Project Licence 70/8165).

334

335 *Animals*

336 Six skeletally mature female Welsh Mountain sheep (3.2 ± 0.8 years, 40-44kg) were included
337 in the study. Experiments were conducted using sterile surgical procedure carried out by the
338 same surgical team. All animals were housed in flocks outside under natural conditions with
339 the same feed, husbandry and location.

340

341 *Animal anesthesia, preparation and surgical technique*

342 Sheep were anaesthetized by intravenous injection of thiopentone (3 mg/kg) and maintained
343 using inhalable anesthetic (a mixture of isoflurane, nitrous oxide, and oxygen). Perioperative
344 analgesia was provided by intramuscular injection of carprofen (4 mg/kg). Antibiotic
345 prophylaxis (procaine penicillin) was given through intramuscular injection. All animals used
346 went through identical surgical procedure under strict aseptic conditions. Each stifle joint was
347 physically examined for abnormality under anesthesia and animals with gross joint instability
348 or pathology was excluded from the study.

349

350 The osteochondral defect (OD) was created on the left stifle joint of experimental sheep. Each
351 animal was placed in a dorsal recumbency position following surgical preparation and the left
352 stifle joint was opened through a parapatellar approach. The patellar fat pad was then elevated
353 to access the medial femoral condyle (MFC) where a 6-mm deep, 8-mm wide OD was created
354 using a hand drill. Following surgery, operated animals were kept in small pens for 48h to
355 reduce ambulation prior to allowing them to fully bear weight. Sheep were then housed in large
356 pens or outdoor fields with normal ambulation before being sacrificed by intravenous injection
357 of 40 ml 20% (w/v) pentobarbitone sodium at 2, 4, and 6-weeks post-surgery. Macroscopic
358 scoring of the joints were carried out by F.H. according to the International Cartilage Repair
359 Society guidelines¹.

360

361 *DRG neuron isolation and culture*

362 Dorsal root ganglia (DRG) were dissected from operated sheep immediately after them being
363 sacrificed with slight modifications from previously performed procedures on sheep and other
364 species²⁻⁴. Sheep were placed on the operating table in the posterior position and their midline
365 fur was shaved using a veterinary clipper. A surgical scalpel was then used to cut open the skin,
366 retract the obliques and latissimus muscles, after which a bone saw was used to remove the
367 lumbar (L2-L5) part of the vertebrae en-bloc. A dorsal laminectomy was then performed using
368 bone saw to expose the spinal cord and DRG (Figure 1B). Exposed DRG were carefully lifted
369 with a forceps while dissecting scissors were used to simultaneously cut the spinal root and
370 peripheral nerve rami to free the DRG.

371 L3 – L4 DRG from contralateral and ipsilateral sides of OD sheep were collected and placed
372 in ice cold dissociation media containing L-15 Medium (1X) + GlutaMAX-1 (Life
373 Technologies) with 24 mM NaHCO₃ supplement. Collected DRGs were then transported back
374 to the laboratory on ice for neuronal isolation. Individual DRG were fully immersed in a 35
375 mm petri dish containing ice cold dissociation media and connective tissues surrounding the
376 DRG were carefully removed using a pair of microscissors. Each DRG was then finely minced
377 into small pieces (3 mm³), submerged in 3 ml collagenase solution (1 mg/ml type I collagenase
378 A (Sigma, UK) with 6 mg/ml Bovine serum albumin (BSA) (Sigma, UK) and placed on a
379 shaker (30 rev/min) for 10 min prior to 15 min incubation in a 37°C incubator. Collagenase
380 solution was then replaced with 3 ml prewarmed trypsin solution (1 mg/ml trypsin (Sigma,
381 UK) with 6 mg/ml BSA in dissociation media) and placed on the shaker for 5 min before 30

382 min incubation at 37 °C. Enzyme solution was then removed and prewarmed culture media
383 (dissociation medium with 10% (v/v) fetal bovine serum, 2% penicillin/streptomycin and 38
384 mM glucose) was added to suspend the DRG. Suspended DRG solution was transferred into a
385 15 ml falcon tube for gentle mechanical trituration with a 1 ml Gilson pipette followed by a
386 brief centrifugation (160 g, 30 s; Biofuge primo, Heraeus Instruments; Hanau, Germany).
387 Supernatant containing dissociated neurons was collected in a fresh tube. This dissociation step
388 was repeated for five times until 10 ml of supernatant was collected. Collected supernatant was
389 centrifuged at 160 g for 5 mins for neuron pelleting, which was then resuspended in 250 µl
390 DRG culture media and plated on Poly-D-lysine and laminin coated glass bottomed dishes
391 (MatTek, P35GC-1.5-14-C) for 3 hours to allow neuron to attach. Additional 2 ml culture
392 media was added to each culture dish following neuron attachment. All neurons were incubated
393 in incubator (37 °C, 5% CO₂) overnight (8 –10 hours) before electrophysiology and calcium
394 imaging recording.

395

396 *Immunohistochemistry*

397 L3 – L4 DRG from contralateral and ipsilateral sides of OD animals were collected as described
398 above. Collected DRG were immediately fixed in Zamboni's fixative (4% paraformaldehyde
399 and picric acid) for 1 hour and transferred to 30% (w/v) sucrose for overnight incubation at
400 4°C. Processed DRG were then embedded in Shandon M-1 embedding matrix (Thermo Fisher
401 Scientific, UK), snap frozen in liquid nitrogen and stored at -80°C. Embedded DRG were
402 sectioned by a Leica Cryostat (CM3000; Nussloch, Germany), mounted on Superfrost Plus
403 microscope slides (Thermo Fisher Scientific) and stored at -20 °C until staining. One to three
404 sections were chosen randomly from both operated and non-operated sides for analysis.
405 Staining was carried by following previous established protocol ⁵ and performed blindly by
406 KW. Anti-CGRP antibody (1:5000, Sigma C8189, anti-rabbit polyclonal), and anti-P2X3
407 antibody (1:1000, Alomone APR016, anti-rabbit polyclonal) following Alexa-488 conjugated
408 secondary antibody (1:1000, Invitrogen A21206, anti-rabbit) and Alexa-568 conjugated
409 secondary antibody (1:500, Invitrogen A-11031, anti-mouse) were used in staining. Mean gray
410 value of each DRG neuron were measured by ImageJ and a custom-made R toolkit
411 (https://github.com/amapruns/Immunohistochemistry_Analysis) was used to score positive
412 neurons with manual validation as previously described ⁵. In brief, a normalized distribution of
413 neurons with the least mean gray value from each section was computed (distribution of
414 minima). All neurons that had a mean gray value greater than 2 standard deviation from the
415 average of the distribution of minima were scored positive.

416

417 *Whole cell patch-clamp Electrophysiology*

418 DRG neuron recordings were made following overnight incubation. At least five neurons from
419 OD or non-operated sides of OD animals (n = 3) were recorded. Neurons were bathed in
420 extracellular solution (in mM): NaCl (140), KCl (4), CaCl₂ (2), MgCl₂ (1), glucose (4),
421 HEPES (10), adjusted to pH 7.4 with NaOH and recorded by EPC-10 amplifier (HEKA)
422 together with Patchmaster© software (HEKA). Glass pipettes used for patching were pulled
423 (P-97, Sutter Instruments) from borosilicate glass capillaries with a resistance of 3–6 MΩ. A
424 ground electrode was placed in the neuron bath to form a closed electric circuit with patching

425 pipette loaded with intracellular solution (in mM): KCl (110), NaCl (10), MgCl₂ (1), EGTA
426 (1), and HEPES (10), adjusted to pH 7.3 with KOH. Neurons were held at -60 mV with pipette
427 and membrane resistance compensated. Resting membrane potential (RMP), cell resistance
428 and capacitance were recorded on current-clamp mode prior than any testing protocols.
429 Neurons with current evoked action potential and a RMP lower than -40 mV were included for
430 analysis. Neuron images were captured by a 40× objective on microscope (Nikon Eclipse Tie-
431 S, Andor) and a Zyla 5.5 sCMOS camera (Belfast, United Kingdom). Cell area was calculated
432 by ImageJ software following pixel to μm conversion.

433

434 Action potentials (AP) were recorded under current-clamp mode without current injection (to
435 record spontaneous firing) following stepwise current injection. Current from 100 pA to 1000
436 pA was injected for 80 ms through 50 steps and the first evoked AP was analyzed. AP
437 threshold, half peak duration (HPD, ms), amplitude, afterhyperpolarization duration (AHP,
438 ms), and afterhyperpolarization amplitude (AHP, mV), were measured using FitMaster
439 (HEKA) software or IgorPro software (Wavemetrics) as previously described⁵.

440

441 Ion channel agonists (capsaicin (1 μM, TRPV1) and α,β, mATP (30 μM, P2X3)) were applied
442 to DRG neurons in a random order through a gravity-driven 12 barrel perfusion system for 10s
443 following 30s ECS wash between stimuli to evoke AP generation under current clamp mode.
444 Both agonist solutions were made up in pH 7.4 ECS from respective stock solution (1mM
445 capsaicin stock in 100% ethanol, Sigma-Aldrich; and 5 mM α,β, mATP stock in 100% ethanol).
446 The average delta spike in response to each agonist was calculated by spike numbers
447 (normalized by subtracting spike numbers at pH 7.4) divided by agonist application time.

448

449 A standard voltage-step protocol was applied on tested neurons under voltage-clamp mode to
450 determine the voltage-current relation⁶. Cells were held at -120 mV for 240 ms before stepping
451 to the test potential (-50 mV to +40 mV in 10 mV increments) for 40 ms (Figure 1H). Voltage
452 was returned to holding potential (-60 mV) for 200 ms between sweeps. Leak subtraction was
453 applied to minimize capacitive currents. Step current density was calculated by minimum
454 (inward) and maximum (outward) current amplitude (pA) (normalised by subtracting average
455 baseline amplitude (100 ms) at -120 mV) dividing cell capacitance (pF). Calculated current
456 density (pA/pF) was then plotted against corresponding step voltage (mV) as voltage-current
457 relation and fitted in Igor Pro using a single or double Boltzmann equation.

458

459 *Ca²⁺ imaging*

460 DRG neurons were incubated in 10 μM Ca²⁺ indicator Fluo-4 AM (diluted from a 10 mM stock
461 solution in DMSO in ECS; Invitrogen, UK) for 30 mins at room temperature (21°C). Neurons
462 were then washed with ECS and placed on microscope (Nikon Eclipse Tie-S, Nikon) for
463 imaging. Fluro-4 fluorescence was excited by a 470 nm LED (Cairn Research) and images
464 were captured by a digital camera (Zyla cSMOS, Andor) at 1 Hz with 50 ms exposure time
465 using Micro-Manager software (v1.4; NIH).

466

467 The same ion channel agonist solutions used in electrophysiology and 50 mM KCl (to serve as
468 a positive control) were applied on neurons following an established perfusion protocol: 10 s
469 ECS wash following 10 s agonist application and another 90 s wash in ECS. All solutions were
470 perfused through a gravity-driven 12-barrel perfusion system. A 3 min interval was applied to
471 allow the neurons to return to their resting state among each perfusion.

472

473 Data analysis was carried following in house protocol⁵. Briefly, KCl positive cells and one
474 black background were draw manually as region of interest (ROI) using ImageJ software and
475 mean gray value of selected ROIs in sequence was extracted. Extracted data were then analyzed
476 by lab-developed R toolbox (<https://github.com/amapruns/Calcium-Imaging-Analysis-with-R>)
477 to calculate Ca²⁺ influx change (normalized to peak KCl response ($\Delta F/F_{max}$) with background
478 subtraction) and the percentage of agonist respondent cells (cells with $\Delta F/F_{max}$ value less than
479 0.001 and peak after 30 s were deleted manually.).

480

481 *Statistics*

482 All figures presented were analyzed and graphed in Graphpad Prism 8 or IgorPro software
483 unless stated otherwise. Data shown as mean \pm Standard Error of Mean (SEM). Two group
484 comparisons were carried by Student's unpaired t-test, and percentage comparison was done
485 by chi-square test. One-way ANOVA (Analysis of Variance) with Tukey post-hoc test was
486 used to compare the significance among three groups. P values less than 0.05 was considered
487 significant.

488

489 **Supplementary Tables**

490 Table 1: scores of osteochondral defects in sheep by ICRS macroscopic scoring system

491

492

Sheep #	ICRS macroscopic score (appearance of joint post mortem)	493
1	3	494
2	2	495
3	2	496
4	2	497
5	3	498
6	2	499

499 Table 2: Action potential properties of sheep DRG neurons in Ctrl and OD groups. * signifies
 500 $p < 0.05$, unpaired t-test.

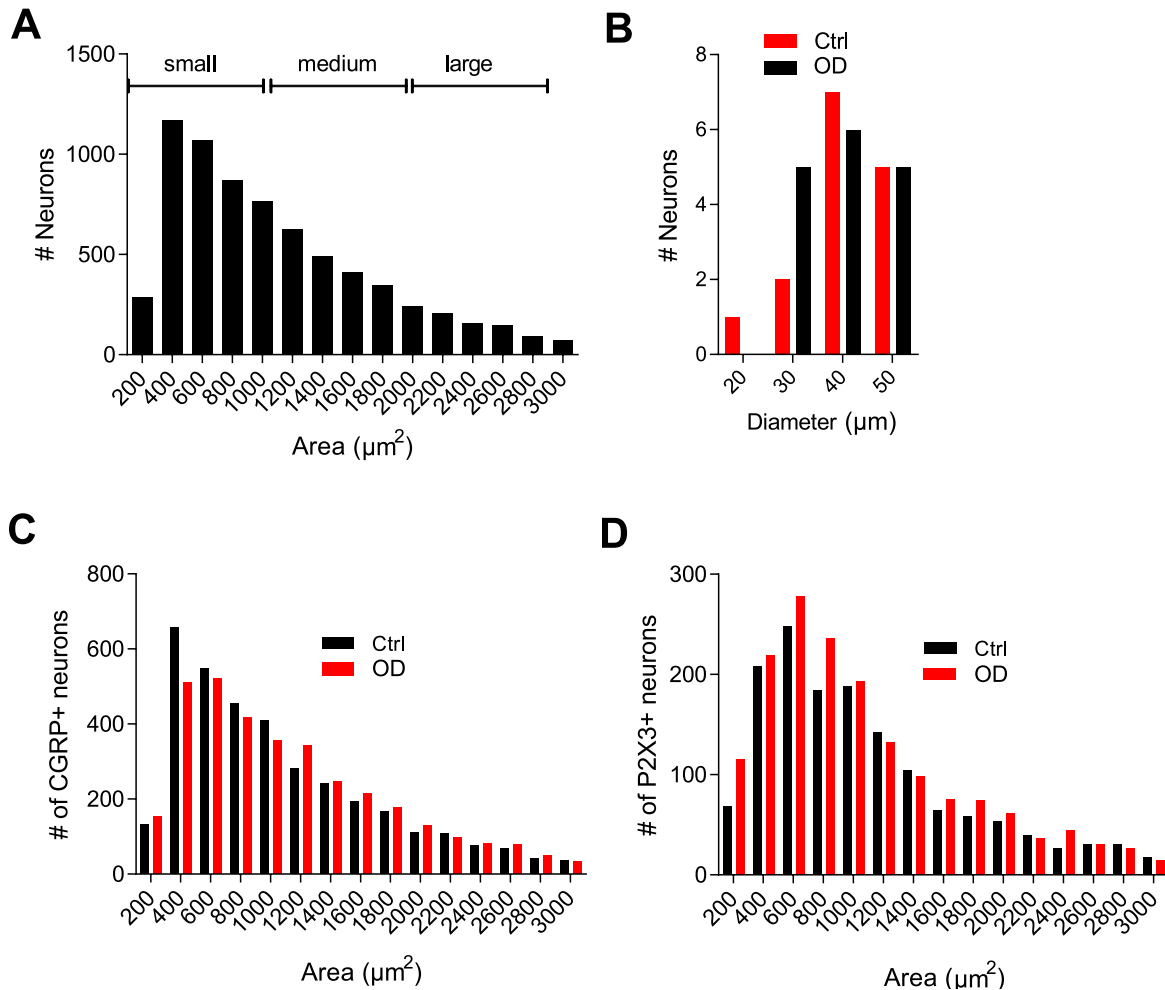
	Ctrl (n = 15)		OD (n = 16)	
	Mean	SEM	Mean	SEM
Diameter (μm)	39.5	2.1	39.5	1.9
Capacitance (pF)	71.0	10.6	80.5	11.9
RMP (mV)	-48.3	3.5	-46.5	2.4
Threshold (pA)	116.7	40.1	100.0	56.5
Half peak Duration (HPD, ms)	3.1*	0.2	4.5	0.5
Afterhyperpolarization duration (AHP, ms)	73.9	9.6	82.7	7.0
Afterhyperpolarization amplitude (AHP, mV)	14.0	1.9	14.0	2.3
Amplitude (mV)	101.6	4.7	103.5	2.8

501

502 Table 3: List of TRPV1 antibodies tested on sheep DRGs

Antibody	Description	Supplier	Cat.
Anti- TRPV1, mouse monoclonal	Primary	Proteintech, UK	66983-1-Ig
Anti-TRPV1, rabbit polyclonal	Primary	Abcam, UK	Ab3487
Anti-Trpv1, rabbit polyclonal	Primary	Abcam, UK	Ab31895
Anti-TRPV1, guinea pig polyclonal	Primary	Alomone	AGP-118

503



504

505 Supplementary figure legend: A) Histogram showing area of each sheep DRG neuron imaged
506 from whole DRG sections and the criteria used in this article for assigning neurons into small,
507 medium and large category. B) Histogram of neuronal diameters on which whole-cell patch
508 clamp was performed. Histograms of cross-sectional areas of neurons stained positive by anti-
509 CGRP (C) and anti-P2X3 (D) antibodies.

510

511 References

- 512 1. van den Borne MPJ, Raijmakers NJH, Vanlauwe J, et al. International Cartilage Repair
513 Society (ICRS) and Oswestry macroscopic cartilage evaluation scores validated for use
514 in Autologous Chondrocyte Implantation (ACI) and microfracture. *Osteoarthritis and*
515 *Cartilage*. 2007;15(12):1397-1402. doi:10.1016/j.joca.2007.05.005
- 516 2. Malin SA, Davis BM, Molliver DC. Production of dissociated sensory neuron cultures
517 and considerations for their use in studying neuronal function and plasticity. *Nature*
518 *Protocols*. 2007;2:152.
- 519 3. Russo D, Clavenzani P, Mazzoni M, Chiochetti R, Di Guardo G, Lalatta-Costerbosa G.
520 Immunohistochemical characterization of TH13-L2 spinal ganglia neurons in sheep

- 521 (Ovis aries). *Microscopy Research and Technique*. 2010;73(2):128-139.
522 doi:10.1002/jemt.20764
- 523 4. Fadda A, Bärtschi M, Hemphill A, et al. Primary Postnatal Dorsal Root Ganglion
524 Culture from Conventionally Slaughtered Calves. *PLOS ONE*. 2016;11(12):e0168228.
525 doi:10.1371/journal.pone.0168228
- 526 5. Chakrabarti S, Pattison LA, Singhal K, Hockley JRF, Callejo G, Smith ESJ. Acute
527 inflammation sensitizes knee-innervating sensory neurons and decreases mouse digging
528 behavior in a TRPV1-dependent manner. *Neuropharmacology*. 2018;143(June):49-62.
529 doi:10.1016/j.neuropharm.2018.09.014
- 530 6. da Silva Serra I, Husson Z, Bartlett JD, Smith ESJ. Characterization of cutaneous and
531 articular sensory neurons. *Mol Pain*. 2016;12:1744806916636387.
532 doi:10.1177/1744806916636387
- 533
- 534